Uninterrupted Connectivity Time in THz Systems Under User Micromobility and Blockage

Dmitri Moltchanov[†], Vitalii Beschastnyi[⋆], Darya Ostrikova[⋆], Yuliya Gaidamaka[⋆‡], and Yevgeni Koucheryavy[†]
[†]Tampere University, Tampere, Finland.
{dmitri.moltchanov, evgeni.kucheryavy}@tuni.fi
[⋆]Peoples' Friendship University of Russia (RUDN University), Moscow, Russia.
{beschastnyy-va, ostrikova-dyu, gaydamaka-yuv}@rudn.ru
[‡]Federal Research Center "Computer Science and Control" of the Russian Academy of Sciences, Moscow, Russia.

***Abstract*—Terahertz (THz) band is considered as the main candidate for new radio access technology in sixth-generation (6G) cellular systems. However, the performance of these systems will be severely affected by not only blockage but user equipment (UE) micromobility in hands of a user. The negative effects of these phenomena can be alleviated by utilizing the multi-connectivity functionality that allows UE to maintain two or more links to nearby base stations (BS) and use them when the currently active link is lost. By accounting for THz specific propagation, antenna and beamsearching design, the density of THz BS deployment, and multi-connectivity operation, we investigate the successful session completion probability under both types of impairments. Our results indicate that the gains of multi-connectivity are observed up to 5 simultaneously supported links and heavily depend on the application outage tolerance time and is mostly affected by micromobility. To improve it, one needs to ensure that the application may tolerate outage caused by beamsearching time which is on the order of milliseconds.**

***Index Terms*—Terahertz communications, micromobility, outage, multi-connectivity, human body blockage, beamsearching**

I. Introduction

Nowadays, when the standardization process of fifth generation (5G) New Radio technology is almost over, the researchers start to explore the new radio interface technology for 6G systems [1], [2]. The common consensus is that this new interface would operate in the lower part of terahertz (THz, $0.3-3$ THz) frequency band [3], [4].

Requiring large antenna arrays at base station (BS) and user equipment (UE) sides to compensate for extreme path losses, THz systems would utilize extremely directional antenna radiation patterns with half-power beamwidth (HPBW) approaching the fraction of a degree [5], [6]. As a side effect, such high directivity allows to efficiently suppress inter-cell interference [7]. However, it also brings a number of unique challenges to system designers. Particularly, in addition to more profound blockage effects as compared to mmWave systems [8], high directivities would lead to frequent outage situations caused by micromobility of UEs, i.e., quick rotations in the user's hands along vertical and transverse axes as well as small displacements along Cartesian axes [9]. As a result of these outages, a beamsearching procedure needs to be invoked to re-establish the active link. The THz link-level performance in presence of UE micromobility impairments has been investigated in [10], where the authors demonstrated principal trade-offs between the fraction of time in outage conditions and achieved link capacity. Depending on the type of impairment, blockage or micromobility, user applications may experience outage periods of different duration affecting session continuity.

One of the ways to avoid blockage in mmWave and THz systems is the use of standardized by 3GPP multi-connectivity functionality [11]. According to it, UE may maintain two or more concurrent connections to nearby BSs and use them once the current link is lost. The multi-connectivity has been studied at the system level in the context of 5G mmWave systems, e.g. [12]–[14]. The use of multi-connectivity for THz systems has been investigated in [15], where the authors demonstrated spectral efficiency and connectivity gains under dynamic blockage impairments. However, this functionality can also be utilized to combat the effects of micromobility.

The studies of multi-connectivity in either mmWave and THz deployments performed so far concentrated on average performance metrics of interest such as outage probability or mean spectral efficiency. However, in practice, the applications utilizing the network often require uninterrupted connectivity to the network ensuring session continuity. However, this problem is significantly more difficult to solve as it requires capturing UE state evolution in time. In this paper, we fill this void by deriving the probability density function (pdf) of the amount of time uninterrupted connectivity time. We explicitly account for THz specific propagation conditions, the density of deployed THz BS, antenna design and beamsearching, as well as the degree of multi-connectivity. Then, by specifying the amount of time an application may spend in outage conditions, we characterize the successful session completion probability.

The main contributions of our study are:

- the mathematical framework for assessment of uninterrupted connectivity time in dense THz BS deployments under user micromobility and blockage impairments in presence of multi-connectivity functionality;
- numerical results illustrating that the session completion probability improves linearly with the degree of multi-connectivity up until 5 simultaneously supported links,

This paper has been supported by the RUDN University Strategic Academic Leadership Program. The reported study has been funded by RFBR, projects 19-07-00933, 20-07-01064.

mostly affected by micromobility, heavily depends on the application outage tolerance time and session duration.

The rest of the paper is organized as follows. First, in Section II we specify our system model. In Section III we introduce our performance evaluation framework and derive the metrics of interest. Numerical results are presented in Section IV while the conclusions are drawn in the last section.

II. System Model

1) Deployment Model: The system model is illustrated in Fig. 1. We assume that THz BSs locations follow Poisson point process (PPP) in $\Re^2$ with the density λ_A. The height of THz BS is h_T. The location of UE of interest is random in the field of BSs implying that the pdf of the distance to the i-s nearest THz BS is [16]

$$f_i(x) = \frac{2(\pi\lambda_A)^i}{(i-1)!} x^{2i-1} e^{-\pi\lambda_A x^2},\ x>0,\ i=1,\dots. \quad (1)$$

2) Propagation and Blockage Models: We assume that line-of-sight (LoS) THz propagation path may suffer from dynamic human body blockage. To capture it, we represent humans by cylinders with base radius r_B and height h_B. The density of blockers is λ_B bl./m^2 and they are assumed to move according to the random direction model (RDM) with the speed v m/s [17]. The UE height is assumed to be h_U, $h_U \le h_B$. Following [18] the time between successive blockage events under RDM is approximately exponentially distributed. Thus, the process of blockage events with i-s BS is Poisson with the mean intensity of $\mu_{B,i}$ provided by

$$\mu_{B,i} = \int_0^\infty f_i(x) \frac{(x[h_B-h_U]+r_B[h_T-h_U])}{(2r_B\lambda_B v)^{-1}(h_T-h_U)} dx. \quad (2)$$

As the effect of human body blockage is known to be more impactful in the THz band [19]–[21], similarly to other studies, e.g., [15], we assume that no communications are feasible in LoS blocked state. The value of SINR at the UE in LoS non-blocked state can be written as [22]

$$S(x) = P_T G_T G_U \left[\frac{x^{-\zeta_T} e^{-Kx}}{N_0}\right], \quad (3)$$

where ζ_T is path loss exponent, N_0 is the thermal noise, P_T is BS emitted power, G_T and G_U are the antenna gains at BS and UE, K is the absorption coefficient [22].

3) Micromobility Model: Following [10], we describe the micromobility process as the Brownian motion with random displacement process over x- and y-planes, and rotations over vertical and transverse axes, $\phi(t)$ and $\theta(t)$. The displacements over z-plane and rotations over longitudinal axis are left out as their contribution to the effect of beam misalignment is negligibly small [10]. This delivers the pdf of the time to beam misalignment, T_A, in the form of the minimum of two random variables (RV) with pdfs corresponding to first passage times of the Brownian particle, i.e.,

$$f_{T_A}(t) = f_\theta(t)[1-F_\phi(t)] + f_\phi(t)[1-F_\theta(t)], \quad (4)$$

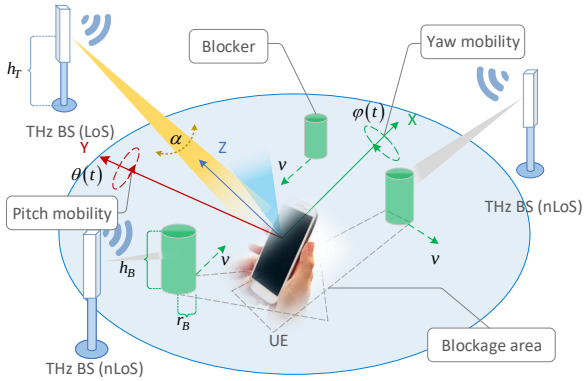

Fig. 1: Illustration of the considered system model.

where the components are provided by

$$f_{(\cdot)}(t) = \frac{M_{\Phi\Theta}}{\sqrt{4\pi D_{(\cdot)} t^3}} \exp\left(-\frac{-M_{\Phi\Theta}^2}{4D_{(\cdot)}t}\right), \quad (5)$$

$D_{(\cdot)}$ is the diffusion constant in appropriate plane set to $\Delta_{(\cdot)}^2/2$, and $M_{\Phi\Theta} = (102\pi/360)(1/N_T + 1/N_U)$, N_U and N_T are the number of antenna elements at THz BS and UE.

4) Antenna Models and Beamsearching Algorithms: We consider square planar antenna arrays at both UE and THz BS. Similarly to [23], [24], we employ a cone radiation pattern model with the beamwidth corresponding to half-power beamwidth (HPBW) of the antenna radiation pattern. Following [25] we approximate the HPBW with $102/N_{(\cdot)}$.

We assume that in the case of LoS blockage or beam misalignment, the THz BSs initiates iterative beamsearching algorithm implemented by sector level sweep and beam refinement procedures, as utilized in, e.g., IEEE 802.11ad/ay systems [26]. The duration of beamsearching procedure is $T_B = (N_U + N_T)\sigma$, where σ is the array switching time.

5) Multi-connectivity Scheme: To evaluate the effect of multi-connectivity on session continuity, we assume that the tagged UE maintains N, $N = 1, 2, \dots$ links to the nearest THz BSs. Since SNR metric is inversely proportional to the distance between the THz BS and UE (3), the nearest BS delivers the best channel quality in terms of time-averaged SNR. The beamsearching procedure is assumed to select a BS with the greatest SNR value at the moment, i.e., the nearest BS in LoS non-blocked conditions. We assume that the beamsearching is invoked at the time when the active connection is lost as a result of micromobility or LoS blockage.

6) Metric of Interest: As opposed to other studies of multi-connectivity, where the authors primarily concentrate on average performance metrics such as outage probability or mean spectral efficiency, we characterize temporal properties of the session service process. Particularly, we first derive the pdf of uninterrupted connectivity time and then use it to express the successful session completion probability.

III. Performance Evaluation Framework

The connectivity and outage intervals in our system organize an alternative renewal process. The idea of our approach is

based on the application of semi-Markov process theory [27] allowing us to characterize an alternating renewal process by the matrix of interval-transient probabilities $\Phi(t)$ consisting of conditional transition probabilities within time t.

To construct the semi-Markov process, we first introduce the chain with states divided into five non-overlapping subsets describing the following states of connectivity, see Fig. 2: (i) active communication with BSs, $j = 1, \cdots, N$ states, (ii) beamsearching due to LoS blockage, $j = N+1, \cdots, 2N$ states, (iii) beamsearching due to micromobility, $j = 2N+1, \cdots, 3N$ states, (iv) outage conditions with continuous connectivity $j = 3N+1, \cdots, 4N$ states and zero state for outage. The states $i = 1, \ldots, N$ correspond to continuous communication periods with i-s BS in LoS conditions.The states $j = N+i, \ldots, 2N$ represent beamsearching procedure due to LoS blockage after association with i-s BS. The introduced absorbing model is characterized by initial vector $\vec{\pi} = [\pi_i]$, $i = 0, ..., 4N$ and matrix of transition probabilities $U = [u_{ij}]$, $i, j = 0, ..., 4N$. We now proceed parameterizing the model and then solve it for pdf of uninterrupted connectivity time.

Recalling the LoS blockage probability with i-s BS [28]

$$p_{N,i} = 1 - \int_0^\infty \frac{2(\pi\lambda_A)^i}{(i-1)!} \frac{x^{2i-1}}{e^{\pi\lambda_A x^2}} e^{-2xr_B\lambda_B \frac{h_B - h_U}{h_A - h_U}} dx, \quad (6)$$

and assuming independence of LoS blockage process, the probability of simultaneous LoS blockage at all the N BSs, i.e., outage condition, can be found as $p_N = \prod_{i=1}^N p_{N,i}$.

Now, we evaluate the temporal characteristics of simultaneous blockage at all N BSs. Following [29] it can be modeled as a busy period in M/GI/∞ system. Let $F_{B,i}(t;x)$ be cumulative distribution function (CDF) of the LoS blocked period with i-s BS that is given by

$$F_{B,i}(t) = 1 - \left(\int_0^t [1 - F_{B,i}(t-z)] \left| de^{-\mu_{B,i} F_T(z)} \right| + \right. \quad (7)$$
$$\left. + [1 - F_T(t)] \left[1 - \int_0^t \frac{1 - F_{B,i}(t-z)}{e^{\mu_{B,i} F_T(z)}} \mu_{B,i} dz \right] \right),$$

where $F_T(t)$ is the CDF of the time elapsed by a single blocker to pass through the UE LoS blockage area. In our model, we consider the rectangular LoS blockage area with the length much greater than its width [30]. This property allows us to assume that the blockers enter the area strictly in a direction orthogonal to the long sides. Thus, the time it takes to cross the LoS blockage zone is $2r_B/v$, which can be written using the Heaviside step function as $F_T(t) = H(t - 2r_B/v)$.

The CDF of the period when all the N BSs are in LoS blocked conditions that follow the connection loss with i-s BS, $T_{NL,i}$, is delivered by the minimum of the LoS blockage periods with all the BS, i.e.,

$$F_{NL}(t;i) = 1 - [1 - F_{B,i}(t)] \prod_{j=1, j\neq i}^N \left[1 - F_{B_j^*}(t) \right], \quad (8)$$

where B_i and B_j^* are the RVs representing blockage and residual blockage periods after continuous association with i-s and j-s BSs, respectively, while $F_{B_i}(x)$ and $F_{B_j^*}(x)$ are the corresponding CDFs. The latter is provided by [29]

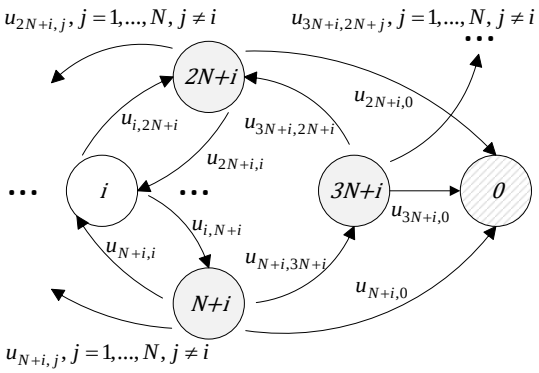

Fig. 2: The absorbing semi-Markov model.

$$F_{B_j^*}(t) = \int_0^\infty \frac{F_{B,i}(t+\tau) - F_{B,i}(\tau)}{\tau[1 - F_{B,i}(\tau)]} d\tau, j = 1, \ldots, N. \quad (9)$$

Now we determine the transition probability metric U of the introduced model in Fig 2. The transition probabilities $u_{2N+i,i}, i = 1, \ldots, N$ corresponding to choosing the same BS after beamsearching procedure triggered by micromobility are conditioned on the fact that the procedure duration is less than outage threshold T_N and none of the $i-1$ nearer BSs are available in LoS non-blocked conditions. We can write

$$u_{2N+i,i} = [1 - F_I(T_B)] \prod_{k=1}^{i-1} p_{N,k}, i = 1, \ldots, N, \quad (10)$$

where $F_I(t) = H(t - T_N)$ is a shifted Heaviside function.

Observe that the choice of other BSs is conditioned on similar requirements given that i-s BS has not been blocked during beamsearching time T_B, i.e.,

$$u_{2N+i,j} = [1 - F_I(T_B)](1 - p_{N,i}) \times$$
$$\times \prod_{k=1, k\neq i}^{j-1} p_{N,k},\ i, j = 1, \ldots, N,\ i \neq j. \quad (11)$$

Recall that the beamsearching procedure can be triggered by either beam misalignment or LoS blockage, providing the conditions for further BS selection. The probability of beamsearching due to beam misalignment should account for the duration of the period to a consequent LoS blockage with the current BS. Thus, we have

$$u_{i,2N+i} = \int_0^\infty \int_y^\infty f_{T_A}(y) f_{T_L,i}(x) dx dy, i = 1, \ldots, N. \quad (12)$$

The probability of beamsearching as a result of LoS blockage is the complementary probability, that is,

$$u_{i,N+i} = 1 - \int_0^\infty \int_y^\infty f_{T_A}(y) f_{T_L,i}(x) dx dy, i = 1, \ldots, N. \quad (13)$$

Summarizing the above-mentioned exposition, the elements of $U = [u_{ij}]$, $i, j = 0, ..., 4N$, can be written as

$$u_{i,N+i} = 1 - \int_0^\infty \int_y^\infty f_{T_A}(y) f_{T_L,i}(x) dxdy, i = 1, \ldots, N,$$
$$u_{i,2N+i} = \int_0^\infty \int_y^\infty f_{T_A}(y) f_{T_L,i}(x) dxdy, i = 1, \ldots, N,$$
$$u_{N+i,j} = (1 - F_I(T_B)) \prod_{k=1}^{j-1} p_{N,k},\ i, j = 1, \ldots, N,\ j \leq i,$$
$$u_{2N+i,i} = (1 - F_I(T_B)) \prod_{k=1}^{i-1} p_{N,k}, i = 1, \ldots, N,$$
$$u_{N+i,3N+i} = (1 - F_I(T_B)) \prod_{k=1, k\neq i}^{N} p_{N,k},\ i = 1, \ldots, N,$$
$$u_{N+i,0} = F_I(T_B),\ i = 1, \ldots, 2N,$$
$$u_{3N+i,2N+i} = F_{NL}(T_N; i) \prod_{k=1}^{i-1} p_{N,k},\ i = 1, \ldots, N,$$
$$u_{3N+i,0} = 1 - F_{NL}(T_N; i), i = 1, \ldots, N,$$
$$u_{0,0} = 1, i = 1, \ldots, N,$$
$$u_{i,j} = 0, \text{ otherwise.} \quad (14)$$

Now, we proceed to derive the metrics of interest. Applying the one-sided Laplace transformation denoted as $f^*(s) = \int_0^\infty e^{-sx} f(x)\, dx$, we obtain the sought matrix in the form

$$\Phi^*(s) = [I - U \circ F^*(s)]^{-1} \Psi^*(s), \quad (15)$$

where U is the transition probability matrix, $F(t)$ is the matrix of pdfs for residence time in state i before transiting to the j-s state obtained further in (16), Ψ is a diagonal matrix with elements $\psi_{ii} = \int_t^\infty \omega_i(t)\, dt$, $\omega_i(t) = \sum_{j=0}^{3N} u_{ij} f_{ij}(t)$ is the residence time in i-s state, $i, j = 0, \ldots, N+1$, and $\circ$ is the Hadamard product of the two matrices.

The elements of $F(t) = [f_{ij}(t)]$, $i, j = 0, ..., 4N$, consisting of transition probabilities within time t can be written as

$$f_{i,N+i}(t) = f_{T_L,i}(t)(1 - F_{T_A}(t)), i = 1, \ldots, N,$$
$$f_{i,2N+i}(t) = f_{T_A}(t)(1 - F_{T_L,i}(t)), i = 1, \ldots, N,$$
$$f_{N+i,j}(t) = \delta(t - T_B), i = 1, \ldots, N,$$
$$f_{2N+i,i}(t) = \delta(t - T_B), i = 1, \ldots, N,$$
$$f_{N+i,3N+i}(t) = \delta(t - T_B), i = 1, \ldots, N,$$
$$f_{N+i,0} = \delta(t - T_N),\ i = 1, \ldots, 2N,$$
$$f_{3N+i,2N+i}(t) = f_{NL}(t; i) F_{NL}(T_N; i), i = 1, \ldots, N,$$
$$f_{3N+i,0}(t) = f_{NL}(t + T_N; i) 1 - F_{NL}(T_N; i), i = 1, \ldots, N,$$
$$f_{i,j}(t) = 0, \text{otherwise}, \quad (16)$$

where $\delta(t)$ is the Dirac delta function. Here, the pdf of the time to LoS blockage at the i-s BS $f_{i,N+i}(t)$ is provided by LoS non-blocked period conditioned on LoS blockage occurring sooner than beam misalignment. On the contrary, $f_{i,2N+i}(t)$ denoting the time to beam misalignment, is conditioned on the complementary event. The constant duration of beamsearching implies that connectivity is resumed in exactly T_B s that is indicated by the shifted Dirac delta function for $f_{N+i,j}(t)$ and $f_{2N+i,j}(t)$, $i, j = 1, \ldots, N$. Similarly, in T_B s the UE may fall into outage conditions, that is captured by $f_{N+i,3N+i}(t)$. Observe that the session is interrupted if the beamsearching lasts longer than T_N, and this is reflected in $f_{N+i,0} = \delta(t - T_N)$. Once the LoS blockage is over, the transition time follows the conditioned pdf to account for the probability $P\{T_{NL} < T_N\} = F_{NL}(T_N; i)$. The transition to the absorbing state is similarly conditioned on the complementary probability $P\{T_{NL} > T_N\} = 1 - F_{NL}(T_N; i)$.

TABLE I: The default system parameters

Notation	Description	Values
λ_A	THz BS density	10^{-3} units/m^2
λ_B	density of blockers	0.3 units/m^2
r_B	blocker radius	0.4 m
h_B	blocker height	1.7 m
h_U	UE height	1.5 m
h_T	THz BS height	4 m
v	blocker speed	1 m/s
P_T	BS emitted power	2 W
ζ_T	path loss exponent in non-blocked state	2.1
K	absorption coefficient	0.2
σ	array switching time	2 μs
T_C	complete session duration	30 s
T_N	tolerable outage period	1 s
N_T	BS antenna array configurations	64x64
N_U	UE antenna array configurations	4x4
N	number of THz BSs	1-10
N_0	density of noise	-84 dBi
$\Delta\theta, \Delta\phi$	mean displacement over vertical and transverse axes	0.1°/s
$\Delta X, \Delta Y$	mean displacement over Ox and Oy	3 cm/s

Utilizing U and F provided in (14) and (16), the diagonal elements of $\Psi^* = \left[\psi_{ij}^*\right]$, $i, j = 0, \ldots, 4N$, are found as

$$\psi_{ii}^*(s) = \frac{1}{s}\left(1 - \sum_{j=0}^{4N} u_{ij} f_{ij}^*(s)\right),\ i = 0, \ldots, 4N,$$
$$\psi_{ij}^*(s) = 0, \text{otherwise}. \quad (17)$$

Once $\Phi^*(s)$ is derived, the reverse Laplace transformation allows us to return to the original matrix of interval-transient probabilities $\Phi(t)$. One needs to perform this step numerically utilizing, e.g., the Talbot algorithm [31], [32]. Then, we determine the pdf of the uninterrupted connectivity time and the probability of successful session completion as follows

$$f_U(t) = 1 - \sum_{i=1}^{4N} \pi_i \Phi_{i0}(t),\ p_U = \int_0^{T_C} f_U(t) dt, \quad (18)$$

where T_C is the complete session duration.

IV. Numerical Assessment

In this section, we present our results by numerically investigating the effect of system parameters on the considered metrics in (18). The default system parameters are provided in Table I.

We start our analysis by illustrating the effect of the degree of multi-connectivity on the probability of successful session completion, p_U, in Fig. 3. Expectedly, the increase in the value of N leads to a higher probability that the session will be

successfully completed. However, as opposed to time-averaged metrics such as outage probability reported in [13] that only gradually improves starting from $N = 3$, here, we observe the gains of utilizing $N = 4$ and $N = 5$. However, starting from $N = 5$ the gains of utilizing additional links diminish.

Different applications may have different outage tolerance times, T_N, i.e., time that they may spend in outage conditions without dropping end-to-end connection. Fig. 4 characterizes the considered metric as a function of session duration, T_C for four considered values of T_N and $N = 1$. Here, $T_N = 5$ ms and $T_N = 5$ s corresponds to extreme cases of highly outage sensitive and insensitive applications, while $T_N = 50$ ms and $T_N = 0.5$ s represents intermediate cases. As one may observe, there is a drastic difference between successful session completion probability for $T_N = 5$ ms and $T_N = 5$ s. The rationale is that in the former case micromobility and blockage both lead to session interruption ($T_B = 0.008224$ s, mean blockage duration for $N = 1$ is 0.96 s) while in the case of $T_N = 5$ s applications may tolerate both blockage and micromobility impairments. It is important that there is no much difference between applications characterized by intermediate values of outage tolerance time, $T_N = 50$ ms and $T_N = 0.5$ s. In spite of the drastic differences in T_N, these applications cannot maintain active connection in case of blockage but are not affected by micromobility. This implies, that adapting future applications to THz access technology one

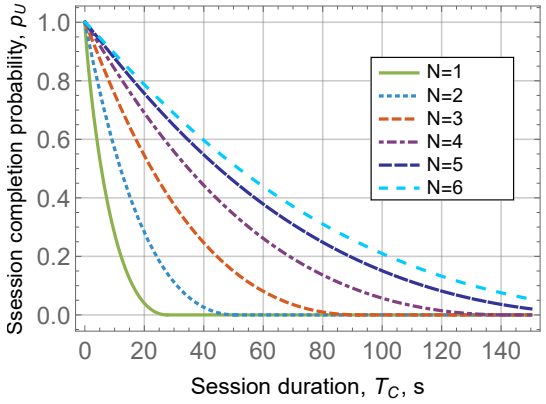

Fig. 3: The effect of the degree of multiconnectivity, N.

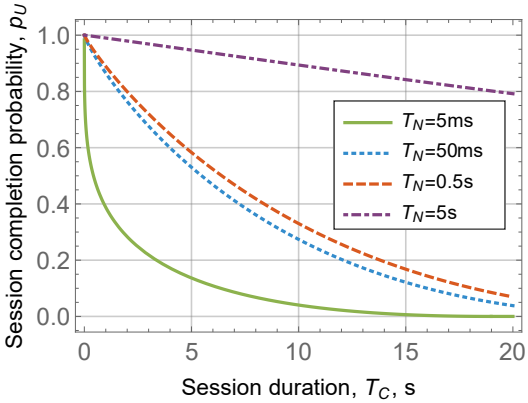

Fig. 4: The effect of outage time tolerance, T_N.

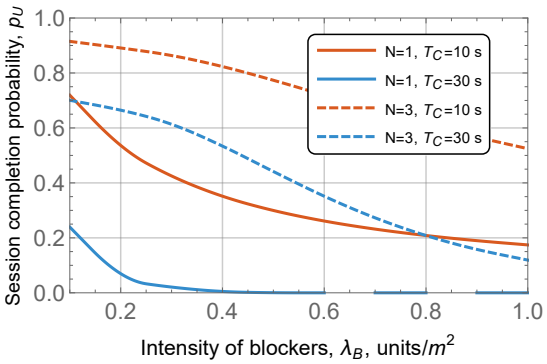

Fig. 5: The effect of blockers intensity, λ_B.

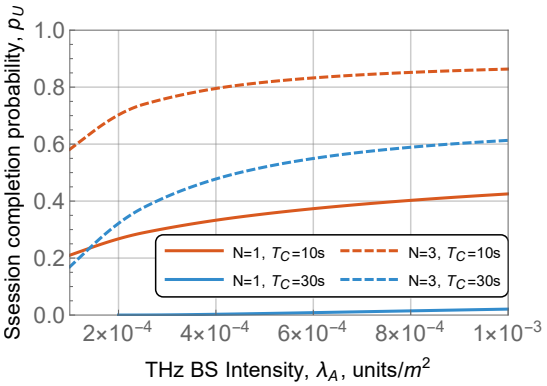

Fig. 6: The effect of THz BS deployment density, λ_A.

needs to ensure that the application can tolerate outage times on the scale of the beamsearching procedure duration.

Consider now the effect of blockers intensity on the successful session completion probability illustrated in Fig. 5 for two degrees of multi-connectivity $N = 1$ and $N = 3$ and two session durations, $T_C = 10$ s and $T_C = 30$ s. Here, we observe that the positive effect of multi-connectivity is preserved across the whole considered range of λ_B. However, the ultimate value of the sought metrics heavily depends on the chosen operational values of N and session duration. Particularly, the curves corresponding to $N = 1$, $T_C = 10$ s and $N = 3$, $T_C = 30$ s are characterized by nearly identical behavior across the considered range of λ_B. Recalling that the use of multiconnectivty may lead to the increased power consumption, this may imply that the choice of the degree of multi-connectivity can be based on the session duration.

Finally, consider the effect of THz BS deployment density, λ_A, on the successful session completion probability illustrated in Fig. 6 for two session durations and two degrees of multi-connectivity. As one may observe, the increase in the THz BS deployment density leads to slight increase in the session completion probability. For example, for $N = 3$ and $T_C = 10$ s, it improves from 0.6 at $\lambda_A = 10^{-4}$ to just 0.82 at $\lambda_A = 10^{-3}$. The rationale is that the use of multi-connectivity functionality in THz systems inherently requires very dense deployments while the distance to nearby BSs at these densities only slightly varies with λ_A. This is in contrast to 5G mmWave BS deployments, where the operational deployment densities for multiconnectivity are much sparser and

thus significant densification gains have been reported [13].

V. Conclusion

In this paper, we investigate the temporal characteristics of the connectivity process in dense THz deployments under dynamic user micromobility and blockage impairments. To this aim, we utilized the semi-Markov framework characterizing the alternative process of connectivity and outage intervals by the matrix of interval-transient probabilities.

We numerically investigated the successful session completion probability as a function of system parameters. Particularly, we have shown that the multi-connectivity gains are observable up to 5 simultaneously supported links. These gains heavily depend on the expected session duration and preserved across the considered range of blockers intensity. The successful session completion probability of applications that are highly sensitive to outage durations is mostly affected by micromobility. In practice, to improve the sought metric, one needs to ensure that the application may tolerate outage caused by beamsearching time which is on the order of milliseconds. Finally, we demonstrated that for practical ranges of THz BS deployment densities, where multi-connectivity can be utilized, no significant densification gains are attained.

References

[1] K. David and H. Berndt, "6G vision and requirements: Is there any need for beyond 5G?," *IEEE Vehicular Technology Magazine*, vol. 13, no. 3, pp. 72–80, 2018.

[2] K. David and H. Berndt, "6G vision and requirements: Is there any need for beyond 5G?," *IEEE Vehicular Technology Magazine*, vol. 13, pp. 72–80, Sep. 2018.

[3] M. Polese, J. M. Jornet, T. Melodia, and M. Zorzi, "Toward end-to-end, full-stack 6G terahertz networks," *IEEE Communications Magazine*, vol. 58, no. 11, pp. 48–54, 2020.

[4] V. Petrov, T. Kurner, and I. Hosako, "IEEE 802.15. 3d: First standardization efforts for sub-terahertz band communications toward 6G," *IEEE Communications Magazine*, vol. 58, no. 11, pp. 28–33, 2020.

[5] Y. Tousi and E. Afshari, "A high-power and scalable 2-D phased array for terahertz cmos integrated systems," *IEEE Journal of Solid-State Circuits*, vol. 50, no. 2, pp. 597–609, 2014.

[6] I. F. Akyildiz and J. M. Jornet, "Realizing ultra-massive mimo (1024× 1024) communication in the (0.06–10) terahertz band," *Nano Communication Networks*, vol. 8, pp. 46–54, 2016.

[7] V. Petrov, M. Komarov, D. Moltchanov, J. M. Jornet, and Y. Koucheryavy, "Interference and sinr in millimeter wave and terahertz communication systems with blocking and directional antennas," *IEEE Transactions on Wireless Communications*, vol. 16, no. 3, pp. 1791–1808, 2017.

[8] B. A. Bilgin, H. Ramezani, and O. B. Akan, "Human blockage model for indoor terahertz band communication," in *2019 IEEE International Conference on Communications Workshops (ICC Workshops)*, pp. 1–6, IEEE, 2019.

[9] V. Petrov, D. Moltchanov, Y. Koucheryavy, and J. M. Jornet, "The effect of small-scale mobility on terahertz band communications," in *Proceedings of the 5th ACM International Conference on Nanoscale Computing and Communication*, pp. 1–2, 2018.

[10] V. Petrov, D. Moltchanov, Y. Koucheryavy, and J. M. Jornet, "Capacity and outage of terahertz communications with user micro-mobility and beam misalignment," *IEEE Transactions on Vehicular Technology*, 2020.

[11] 3GPP, "NR; Multi-connectivity; stage 2 (Release 16)," 3GPP TS 37.340 V16.0.0, December 2019.

[12] M. Polese, M. Giordani, M. Mezzavilla, S. Rangan, and M. Zorzi, "Improved handover through dual connectivity in 5G mmWave mobile networks," *IEEE Journal on Selected Areas in Communications*, vol. 35, pp. 2069–2084, Sept. 2017.

[13] M. Gapeyenko, V. Petrov, D. Moltchanov, M. R. Akdeniz, S. Andreev, N. Himayat, and Y. Koucheryavy, "On the degree of multi-connectivity in 5G millimeter-wave cellular urban deployments," *IEEE Transactions on Vehicular Technology*, vol. 68, no. 2, pp. 1973–1978, 2019.

[14] V. Begishev, E. Sopin, D. Moltchanov, R. Pirmagomedov, A. Samuylov, S. Andreev, Y. Koucheraryvy, and K. Samouylov, "Performance Analysis of Multi-Band Microwave and Millimeter-Wave Operation in 5G NR Systems," *IEEE Transactions on Wireless Communications*, 2021.

[15] A. Shafie, N. Yang, and C. Han, "Multi-connectivity for indoor terahertz communication with self and dynamic blockage," in *ICC 2020-2020 IEEE International Conference on Communications (ICC)*, pp. 1–7, IEEE, 2020.

[16] D. Moltchanov, "Distance distributions in random networks," *Elsevier Ad Hoc Networks*, vol. 10, pp. 1146–1166, August 2012.

[17] P. Nain, D. Towsley, B. Liu, and Z. Liu, "Properties of random direction models," in *IEEE 24th Annual Joint Conference of the IEEE Computer and Communications Societies*, vol. 3, pp. 1897–1907, March 2005.

[18] V. Begishev, D. Moltchanov, E. Sopin, A. Samuylov, S. Andreev, Y. Koucheryavy, and K. Samouylov, "Quantifying the impact of guard capacity on session continuity in 3GPP new radio systems," *IEEE Transactions on Vehicular Tech.*, vol. 68, no. 12, pp. 12345–12359, 2019.

[19] T. Kürner, A. Fricke, S. Rey, P. Le Bars, A. Mounir, and T. Kleine-Ostmann, "Measurements and modeling of basic propagation characteristics for intra-device communications at 60 GHz and 300 GHz," *Journal of Infrared, Millimeter, and Terahertz*, vol. 36, no. 2, pp. 144–158, 2015.

[20] N. Khalid and O. B. Akan, "Wideband THz communication channel measurements for 5G indoor wireless networks," in *2016 IEEE International Conference on Communications (ICC)*, pp. 1–6, IEEE, 2016.

[21] V. Petrov, J. M. Eckhardt, D. Moltchanov, Y. Koucheryavy, and T. Kurner, "Measurements of reflection and penetration losses in low terahertz band vehicular communications," in *2020 14th European Conference on Antennas and Propagation*, pp. 1–5, IEEE, 2020.

[22] P. Boronin, V. Petrov, D. Moltchanov, Y. Koucheryavy, and J. M. Jornet, "Capacity and throughput analysis of nanoscale machine communication through transparency windows in the terahertz band," *Nano Communication Networks*, vol. 5, no. 3, pp. 72–82, 2014.

[23] V. Petrov, M. Komarov, D. Moltchanov, J. M. Jornet, and Y. Koucheryavy, "Interference and SINR in millimeter wave and terahertz communication systems with blocking and directional antennas," *IEEE Transactions on Wireless Communications*, vol. 16, pp. 1791–1808, March 2017.

[24] E. Mokrov, A. Ponomarenko-Timofeev, I. Gudkova, P. Masek, J. Hosek, S. Andreev, Y. Koucheryavy, and Y. Gaidamaka, "Modeling transmit power reduction for a typical cell with licensed shared access capabilities," *IEEE Vehicular Technology Magazine*, vol. 67, no. 6, pp. 5505–5509, 2018.

[25] A. B. Constantine *et al.*, "Antenna theory: analysis and design," *Microstrip Antennas, John Wiley & Sons*, 2005.

[26] IEEE, "Telecommunications and information exchange between systems local and metropolitan area networks – specific requirements. Part 11. Amendment 3," IEEE standard for information technology, 2012.

[27] E. Cinlar, "Markov renewal theory," *Advances in Applied Probability*, vol. 1, no. 2, pp. 123–187, 1969.

[28] M. Gerasimenko, D. Moltchanov, M. Gapeyenko, S. Andreev, and Y. Koucheryavy, "Capacity of multiconnectivity mmwave systems with dynamic blockage and directional antennas," *IEEE Transactions on Vehicular Technology*, vol. 68, no. 4, pp. 3534–3549, 2019.

[29] M. Gapeyenko, A. Samuylov, M. Gerasimenko, D. Moltchanov, S. Singh, M. R. Akdeniz, E. Aryafar, N. Himayat, S. Andreev, and Y. Koucheryavy, "On the temporal effects of mobile blockers in urban millimeter-wave cellular scenarios," *IEEE Transactions on Vehicular Technology*, available online, 2017.

[30] M. Gapeyenko, A. Samuylov, M. Gerasimenko, D. Moltchanov, S. Singh, E. Aryafar, S.-p. Yeh, N. Himayat, S. Andreev, and Y. Koucheryavy, "Analysis of human-body blockage in urban millimeter-wave cellular communications," in *Communications (ICC), 2016 IEEE International Conference on*, pp. 1–7, IEEE, 2016.

[31] A. M. Cohen, *Numerical methods for Laplace transform inversion*, vol. 5. Springer Science & Business Media, 2007.

[32] A. Ometov, D. Kozyrev, V. Rykov, S. Andreev, Y. Gaidamaka, and Y. Koucheryavy, "Reliability-centric analysis of offloaded computation in cooperative wearable applications," *Wireless Communications and Mobile Computing*, vol. 2017, pp. 1–15, 2017.